ISSN 2816-8089

RESEARCH ARTICLE

Identification of Unique Water Molecules in Human GRK2 Protein with Bound and Unbound GβGγ Subunit: A Study by Structural Bioinformatics Method

Hridoy Ranjan Bairagya*, Sayanti Pal, Sabarno Baral

Computational Drug Design and Bio-molecular Simulation Lab, Department of Bioinformatics, Maulana Abul Kalam Azad University of Technology, West Bengal 741249, India.

Abstract

The human G-protein coupled receptor kinase 2 (hGRK2) regulates the desensitization of beta-adrenergic receptors (β-AR), and its overexpression has been implicated in heart failure. The hGRK2 is a serine/ threonine kinase and is one of the members of the AGC family, and it contains the four domains (i) RGS or RH domain (regulator of G-protein signaling res. id. 54-175), (ii) protein kinase or CAT domain (res. id. 191-453), (iii) AGC Kinase domain (res. Id 454-521), and (iv) PH domain (Pleckstrin homology, res. Id. 558-652). Present computational investigations on multiple analyses of X-ray structures (bound and unbound conformation of $G_\beta G_\gamma$) highlight the presence of seventeen unique water molecules (W1 to W17) that are only available either in hGRK2 with $G_\beta G_\gamma$ or without $G_\beta G_\gamma$. These water molecules are subdivided into category-I (W1 to W8), which is observed with unbound $G_\beta G_\gamma$ conformation, and category-II (W9 to W17) in hGRK2 with bound $G_\beta G_\gamma$ conformation. The MD simulation results suggest the non-crystal and crystal water molecules are inaccessible to reaching W3, W10, and W12 water sites because they are deeply buried and shielded by neighboring residues, whereas W9, W11, and W13 are accessible by crystal water in MD simulation but not allow entering non-crystal or MD water molecules. During the structural transition of hGRK2 from unbound to bound $hG_\beta G_\gamma$ state, water molecules of category-I (W1 to W8) departed from their respective domains, and water molecules of Category-II (W9 to W17) were reached simultaneously during unbound to bound $G_\beta G_\gamma$ conformation. In this context, the present work identifies new biochemical insights to highlight some rationale clues for heart disease.

Key Words: *hGRK2; $G_\beta G_\gamma$; Unique water molecules; Structural transition; Water dynamics*

***Corresponding Author**: Hridoy Ranjan Bairagya, Associate Professor, Computational Drug Design and Bio-molecular Simulation Lab, Department of Bioinformatics, Maulana Abul Kalam Azad University of Technology, West Bengal 741249, India; E-mail: hbairagya@gmail.com*

***Received Date**: June 12, 2023, **Accepted Date**: July 11, 2023, **Published Date**: July 21, 2023*

***Citation**: Bairagya HR, Pal S, Baral S. Identification of Unique Water Molecules in Human GRK2 Protein with Bound and Unbound GβGγ Subunit: A Study by Structural Bioinformatics Method. Int J Bioinfor Intell Comput. 2023;2(2):184-211.*

1. Introduction

The mammalian GRKs are Serine/Threonine Kinases that are categorized into three subfamilies which include the GRK1 (further grouped into GRK1 and GRK7), the GRK2 (further grouped into GRK2 and GRK3) and the GRK4 (further grouped into GRK4, GRK5 and GRK6) [1]. The hGRKs are expressed at various levels and are responsible for multiple pathophysiological conditions in the human system. However, the hGRKs have multiple functional domains, which include an N-terminal alpha (αN) (res. Id. 1 to 17), an N-terminal RH (res. Id. 39 to 184), a central catalytic Kinase Domain (KD) (res. Id. 185 to 454), AGC C-Tail (res. Id. 455 to 512), and a C-terminal RH domain (res. Id. 513 to 546). Moreover, an extra Pleckstrin Homology (PH) domain (res. Id. 547 to 665) is also found at the C-terminal of the native GRK2 protein [2]. This active $G_{\beta}G_{\gamma}$ complex, in association with native GRK2, brings the protein toward the G-Protein Coupled Receptors (GPCRs), one of the most prominent families of cell surface receptors for the phosphorylation of its cytoplasmic loop to adopt various extracellular signals [3].

GPCRs are seven-transmembrane proteins in the eukaryotic genomes, including an N-terminus at the extracellular region and a C-terminus incorporated in the extracellular region of the Plasma membrane (PM) [4]. The extracellular region interacts with ligands whereas; the C-terminus in the intracellular region is associated with the G-Protein having three subunits, the G_{α}, G_{β}, and G_{γ} [5]. The GPCR undergoes a conformational change upon ligand binding and is activating the G-protein subunits. The G_{α} subunit is known to have its own GTPase activity, whereas the G_{β} and G_{γ} remain together as a $G_{\beta}G_{\gamma}$ complex which recruits the GRK protein by attaching itself to the PH domain [6]. In the case of GRK subfamilies other than GRK2, the PH domain is absent; the attachment of the $G_{\beta}G_{\gamma}$ complex occurs through the palmitoylation of the C-terminal region of the protein. The C-tail of AGC region gets attached to the cytoplasmic loop and phosphorylates a set of serine/threonine residues in the cytoplasmic loop region of GPCRs. Various structures have been investigated under hGRK2 [7,8], and the samples have been obtained from different species such as hGRK2 without $hG_{\beta}G_{\gamma}$ Figure 1 or with $hG_{\beta}G_{\gamma}$ Figure 2 or bovine $G_{\beta}G_{\gamma}$ which are taken as initial samples for the present investigational study.

Recently, many reports have indicated that G protein-coupled receptors (GPCR), and related enzymes play an important role in cardiovascular disease. However, up or down-regulation of GRK2 may occur in several pathophysiological disorders, and these changes can cause cardiovascular and metabolic diseases. Thus, GRKs are one of the most significant drug targets, and the search for a potent molecule to inhibit the activity of GRKs has become quite tricky. Furthermore, genetic inhibition is considered as one of the most powerful therapies to treat abnormalities related to GRK proteins. The first compounds, polyanionic and polycationic, such as heparin that could bind with GRK2, negatively impacted the GRK2 activity [9]. In addition, small molecule inhibition of GRKs demonstrate better efficacy in treating diseases caused by GRKs, and one such small molecule is paroxetine, which has claimed effective inhibition against GRK2 and improved cardiac dysfunction [10].

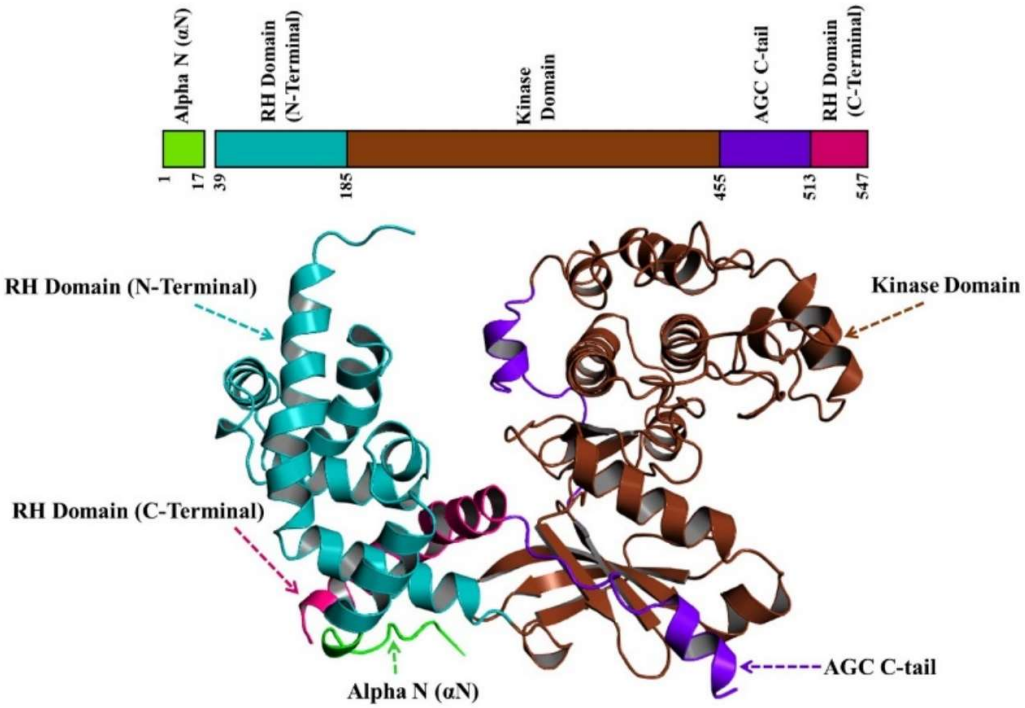

Figure 1: *The structural overview of human GRK2 with unbound $G_\beta G_\gamma$ (PDB Id: 5UVC). All the respective domains (without PH domain) are marked with different colour.*

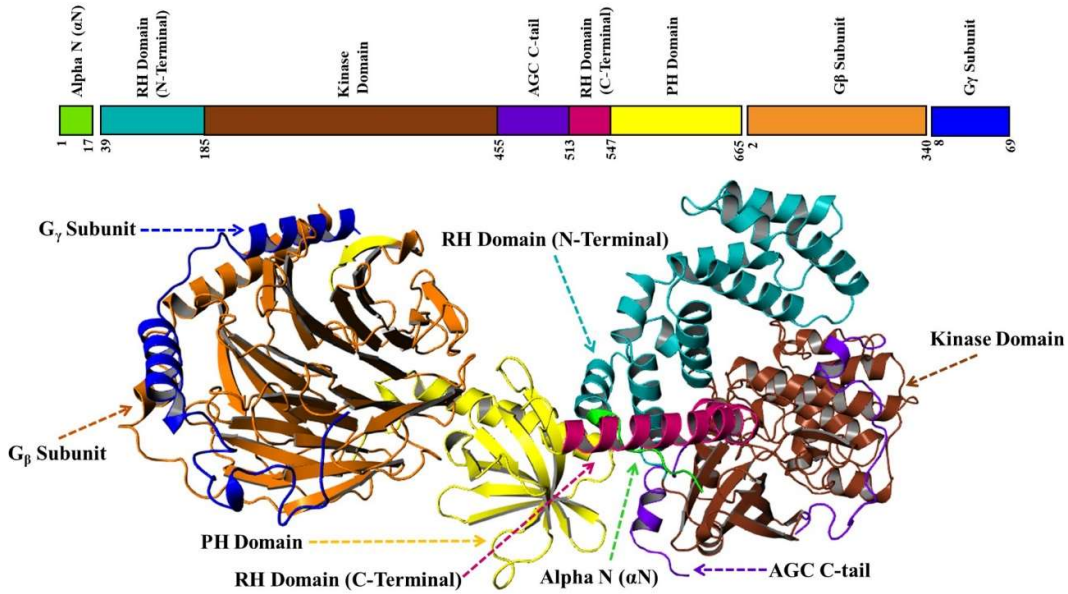

Figure 2: *The structural overview of human GRK2 with bound $G_\beta G_\gamma$ (PDB Id: 5UKL). All the respective domains are marked with different colour.*

Water molecules have been known to play a pivotal role in protein structure, enzyme catalysis, protein architecture, conformational stability, protein plasticity, stabilization of salt bridges, and ligand binding process [11]. In spite of relevance of water molecules, we do suggest high-resolution X-ray structures of hGRK2 highlights insufficient insights about the

structural and functional importance of conserved water molecules in the aspect of the water binding pocket. Thus, high-resolution crystal structures of hGRK2 cannot yield dynamical details regarding the geometrical position of water molecules, whereas water dynamics techniques can extract the structural and dynamical information of protein that is inaccessible in experimental study. Due to the poor electron density of protein crystal, the prediction and visualization of water molecules in the structure are really challenging; therefore, most computational studies ensure to pay more attention to their vital role. Specifically, water dynamics simulations with explicit water solvent seem like a promising approach for the investigation of the water sites in protein structures.

These water sites (W) of hGRK2 protein are defined as confined space regions close to the residues of the protein surface, exhibiting a high probability of hosting water molecules. The positions of water sites, W, are chosen by the coordinates of the maximum probability point using a surface residue of the protein as a reference that can make H-bonds favorably with the water molecules [12]. During the past few years, computational studies propose the relevance of conserved water molecules and support the idea that the displacement of these water molecules should have a crucial effect on binding energy [13,14]. As a result, these phenomena of water displacement may be considered for the implementation of water-based drug discovery techniques in heart disease. Thus, we expect that our study of the entry and exit process of some signature water molecules may extract relevant information about the binding and unbinding biochemical mechanism of $G_{\beta}G_{\gamma}$ subunits with GRK2 protein. The results may also advance our understanding of how conformational transitions of hGRK2 influence its biological functionality.

Different researchers have considered human GRK2 as a significant drug target; hence they adopt various computational strategies to investigate some promising selective inhibitors for GRK2 to treat heart failure [15,16]. Moreover, no detailed computational investigation has yet been reported for evaluating the following information:

1. Identifications of conserved water molecules in the in-X-ray structures of human GRK2.
2. Comparative analysis of water molecules between crystal and MD structures.
3. Investigation of the binding mechanism $G_{\beta}G_{\gamma}$ with hGRK2 and its effect on the entry or exit of unique conserved water molecules from GRK2 protein.

To our knowledge, this is the first computational report incorporating the results of water dynamics analysis and focused on identifications of seventeen (W1 to W17) conserved water molecules. Multiple analyses of the human GRK2 protein crystal structures provide suggestions for displacing water molecules. Hence, our computational study may be extended biochemical information about the association and dissociation mechanism of GRK2 protein with $G_{\beta}G_{\gamma}$ that links the experimental investigations and provide a testable hypothesis for validation.

2. Material and Methods

2.1. Structure collection

To investigate the role of domain-bound water molecules in human GRK2 protein, eighteen human GRK crystal structures were obtained from the Protein DataBank (PDB) [17]. The

research work was emphasized between the comparative analysis of water molecules in human GRK2 with category-II (bound $hG_{\beta}G_{\gamma}$) and category-I (unbound $hG_{\beta}G_{\gamma}$ form). The PDB Id 5UKL and 5UKK of human GRKI contain bound $hG_{\beta}G_{\gamma}$ and 5UVC and 5UUU with unbound $hG_{\beta}G_{\gamma}$. The crystal structures with low solvent content diffract better than those with high resolution. Hence, crystal structures 5UKL and 5UVC are higher resolutions and solvent concentrations; they are considered a template for present structural and dynamic analysis.

2.2. Identification of conserved water molecules inhuman GRK

Eight conserved water molecules (W1 to W8) were identified at the different domains of hGRK2 with bound $hG_{\beta}G_{\gamma}$ crystal structures and nine (W9 to W17) in unbound $hG_{\beta}G_{\gamma}$ using the 3-Dimensional Structural Superposition (3dSS) program (http://cluster.physics.iisc.ernet.in/3dss/) [18]. However, the above mentioned seventeen conserved water molecular positions were also verified by the Swiss PDB Viewer program [19]. Two water molecules (oxygen atoms) or two atoms (oxygen atoms between two water molecules or oxygen atom of the water molecule and specific atom of ligand) whose center-to-center distance was within 1.80Å, [20,21], in between reference (PDB Id: 5UVC in category-I and 5UKL in Category-II), and movable structures; that were assigned as conserved [22-24]. Each conserved water molecule also makes at least one H-bond with protein molecules. The unique conserved water molecules present either 5UKL or 5UVC crystal structures.

2.3. Calculation of water mobility and SASA

The normalized B-factor (Å^2) for seventeen conserved water molecules were calculated using the z-score for filtering out the outliers in raw B-factor values (Equation 1).

$$B_{NORM} = \frac{B_i - \langle B \rangle_p}{\sigma(B)} \quad [1]$$

Where B_i is each protein atom's B-factor, $\langle B \rangle_p$ is the protein molecule's mean B-factor, and (B) is the standard deviation of the B-factors is used to determine the mobility of the twenty-one conserved water molecule [25,26]. A python library (MD-Analysis) was used to calculate the normalized B-factor of the twenty-one conserved water molecules (https://doi.org/10.25080/Majora-629e541a-00e), and their solvent accessible surface area (SASA) was calculated using an in-house TCL script with a probe radius of 1.40 Å. Water molecules that had the SASA value of less than or equal to 2.50 Å^2 were assigned to be buried. The side-chain accessibility surface area (ASA) of reference residues of each of the twenty-one conserved water molecules was calculated using the Get Area web server.

2.4. Reconstruction of disordered regions of human GRK X-ray structures

The X-ray structures of 5UKL and 5UVC have several disordered regions characterized by poor electron density. The sequence of these disordered regions in each system was obtained from the Protein Data Bank, and these missing residues or amino acid sequences were integrated into the 5UKL (Ile485 to Gly495) and 5UVC (Thr97 to Arg101, Cys120 to Val141, Glu476 to Leu498, and Glu537 to Ala538) crystal structures. Initially, each residue was added in the appropriate gaps of each structure and refined using the GROMOS 36 force field [27] of the Swiss PDB Viewer program. Energy minimization was performed using 250 steps of

steepest descent followed by 500 cycles of conjugate gradient without any constraints [28,29]. Then the added residue was allowed to move freely until its conformations were stereo-chemically compatible. Similarly, all missing residues were incorporated or appropriately fitted in the disordered regions of their respective PDB structures in 5UKL and 5UVC. The entire model structure was again energy minimized (500 steps of steepest descent followed by 1000 cycles of conjugate gradient) until the energy charges decreased to 0.001 kJ/mol, for a 10.00 Å cutoff distance in the non-bonded interaction, with a distance dependent dielectric constant.

2.5. Model evaluation for human GRK

Verification of the final structures of 5UKL and 5UVC was performed by the Structural Analysis and Verification Server (UCLA-DOE LAB - SAVES v6.0SAVES) program-[30]. The structural quality (Pro-check) [31],-stereochemical parameters of residues (What Check), non-bonded interactions (Errat) [32], energy profile or Z-score (ProSA using molecular mechanics force field), and identification of unreliable portions (Verify-3D) [33,34] in each predicted model of the disordered regions were thoroughly checked and calibrated. The Z-score and environmental score (Verify-3D) of added residues in the disordered regions of 5UKL and 5UVC were between -12.14 and -9.66, respectively. In addition, 98% of these residues occupied the favourable allowed region in the Ramachandran plot [35]. The structures were further validated by homology modeling using the SWISS-MODEL program [36]. The predicted disordered regions of each structure had also been checked by model assessment tools, which verified local and global quality, stereochemistry, and structural features of the modelled region.

2.6. Calculation of pKa values of the ionizable residues

The pKa values and protonation states of seventeen titratable residues in 5UKL and 5UVC crystal structures were determined using the Protein Prepare application module of the PlayMolecule program [37]. The Protein Prepare program calculates the pK_a values of the side chains of those titratable residues using an empirical method PROPKA (version 3.1) at pH 6.00. In order to investigate the validation of the method described above, we also measured the pK_a values of those corresponding titratable residues in 5UKL and 5UVC crystal structure sare compared the pK_a values with 5UKL and 5UVC structures, respectively Table S1.

2.7. Molecular dynamics simulations and trajectory analysis

The model 5UKL and 5UVC structures at pH 6.0 were prepared for further water dynamic studies in the presence or absence of crystal water molecules to identify the conserved water molecules at hGRK protein to evaluate their structural properties. Using the AutoPSF module of the Visual Molecular Dynamics (VMD v.1.9.3.) program, missing hydrogen atoms were added to each structure. Each structure was then solvated with the presence and absence of crystal water molecules in a cubic box of around 9,000 TIP3P water molecules extending at least 5 Å from the protein surface. Sodium and chloride ions were employed to neutralize the overall charge of the system; the resulting system consisted of around 150000 atoms. MD simulation was performed for the 5UKL and 5UVC structure using the Nano-scale Molecular Dynamics (NAMD v.2.11) program [38] by assigning the CHARMM-36all-atom force field (with map correction) for protein. The energy minimizations were adopted to stabilize the

system using the steepest-descent method by 5000 steps. Then each system was equilibrated by fixing protein atoms for 10ns under *NPT* [39,40]. To mimic physiological conditions, the temperature was kept at 310 K using Langevin dynamics with a damping coefficient 5 ps-1. The pressure was maintained at 1 atm using the Langevin piston Nose-Hoover method, with a piston period of 100 fs and a decay time of 50 fs.

During the water dynamics, Nos´e-Hoover Langevin piston barostat and Langevin thermostats [41] were used to enforce constant pressure and temperature. The SHAKE algorithm [42] was used to keep bonds involving H atoms at their equilibrium length, allowing a 2 fs time step. The van der Waals interactions were truncated at 12.0 Å with switching from 10.0 Å. Electrostatic interactions were modelled accordingly with a dielectric Constant of 1.0 throughout the equilibration and production runs. The standard Particle-Mesh Ewald method was used with periodic boundary conditions to compute the long-range electrostatic interaction of the system by specifying an appropriate Particle-Mesh Ewald grid size. Finally, each structure's production runs of water dynamics were performed in the NPT ensemble for 10 ns. The atomic coordinates were recorded at every 2 ps for further data analysis (5,000 frames). Each MD trajectory, especially 5000 recorded snapshots, was considered for further data analysis using the VMD program.

3. Results and Discussion

The eighteen crystal structures of the human GRK2 protein were obtained from the Protein Data Bank. Several research groups (C1 2 1) have independently solved these structures using PHENIX and REFMAC refinement programs at different (4.6 to 7.0) pH levels and different resolutions (2.07 to 3.15) Table 1. The PDB Id 5UVC and 5UUU of category-I with unbound $hG_{\beta}G_{\gamma}$ and 5UKL and 5UKK of category-II with bound $hG_{\beta}G_{\gamma}$ revealed the existence of seventeen (IW1 to IW17) water molecules at the different domains of the human GRK2 protein, which may have alleged roles in the structure, function, and stabilization of the GRK2 protein**.** The corresponding water molecule of IW1 is W702, IW2 for W703, IW3 for W707, IW4 for W709, IW5 for W715, IW6 for W716, IW7 for W734, IW8 for W754 IW9 for W810, IW10 for W814, IW11 for W839, IW12 for W860, IW13 for W866, IW14 for W876, IW15 for W891, IW16 for W928, and IW17 for W931 Table 2. Furthermore, the superimposed complexes between 5UVC and 5UUU from category-I and 5UKL and 5UKK from category-II have displayed the presence of IW1 to IW8 unique conserved water molecules in category-I and IW9 to IW17 in category-II Figure 3.

These water molecules are only in unbound or bound $hG_{\beta}G_{\gamma}$ conformation at GRK2 protein Table 2. Interestingly, the structural position of IW1 from category-I and IW10 from category II is very stable as their B-Factor values are 25.92 $Å^2$ and 33.58 $Å^2$, respectively; on the contrary, IW3 from I and IW15 from II are more unstable with B-factor 65.52 $Å^2$ and 45.73 $Å^2$ Tables 3 and 4. According to a suggestion from [43],if B-Norm is greater than or equal to 1.20 $Å^2$ for any hydration site, the water molecule will be fully occupied. This information indicates water molecules of category-I and II are not fully occupied. However, IW1 has four center H-bonds, whereas IW10, IW3, and IW15 have three Figures 4 and 5.

Table 1: *List of X-ray structures of human GRK protein and their crystallographic structural parameters.*

PDB ID	Classification	Method	Resolut-ion (Å)	R value free/ R value work	Space group	pH/ sequence length	Refinem-ent methods	Unit Cell	
								Length (Å)	Angle (∘)
3CIK	Signalling protein	X RAY DIFF	2.75	0.26/0.20	C 1 2 1	5.25/689	REFMAC	a=185.73 b=73.60 c=122.91	α=90 β=155.22 γ=90
3KRW	PROTEIN BINDING	X RAY DIFF	2.90	0.26/0.21	C 1 2 1	NA/688	REFMAC	a=182.35 b=73.522 c=121.21	α=90 β=114.26 γ=90
3KRX	PROTEIN BINDING	X RAY DIFF	3.10	0.27/0.23	C 1 2 1	NA/688	REFMAC	a=182.07 b=73.2 c=121.7	α=90 β=114.51 γ=90
3V5W	Transferase/ Transferase inhibitor	X RAY DIFF	2.07	0.24/0.19	C 2 2 21	5.8 /689	REFMAC	a=194.97 b=71.01 c=111.16	α=90 β =110.41 γ=90
4MKO	Signalling protein	X-RAY DIFF	2.40	0.23/0.17	C 2 2 21	4.6/640	REFMAC	a=61.22 b=240.97 c=212.08	α=90 β=90 γ=90
4PNK	Transferase/ Transferase inhibitor	X RAY DIFF	2.56	0.25/0.19	C 2 2 21	7.0/689	REFMAC	a=61.43 b=241.39 c=212.52	α=90 β =90 γ=90
5HE1	Transferase/ Transferase inhibitor	X RAY DIFF	3.15	0.25/0.16	C 2 2 21	6.0/642	REFMAC	a=62.02 b=241.36 c=212.9	α=90 β =90 γ=90
5UKK	Transferase/ Transferase inhibitor	X RAY DIFF	2.60	0.28/0.22	C 1 2 1	6.0/642	REFMAC	a=113.12 b=63.42 c=102.03	α=90 β =92.81 γ=90
5UKL	Transferase/ Transferase inhibitor	X RAY DIFF	2.15	0.22/0.18	C 1 2 1	6.0/642	REFMAC	a=194.25 b=71.42 c=111.25	α=90 β=110.51 γ=90
5UUU	Transferase/ Transferase inhibitor	X-RAY DIFF	2.7	0.25/0.21	P 31 2 1	5.60/547	REFMAC	a=126.18 b=126.18 c=96.369	α=90 β=90 γ=120
5UVC	Transferase/ Transferase inhibitor	X-RAY DIFF	2.65	0.26/0.21	P 42 21 2	5.90/547	REFMAC	a=113.15 b=113.15 c=95.42	α=90 β=90 γ=90

5WG3	Transferase/ Signalling Protein	X RAY DIFF	2.90	0.24/0.19	C 2 2 21	6.0/689	PHENIX	a=61.26 b=241.56 c=214.81	α=90 β =90 γ=90
5WG4	Transferase/ Signalling Protein	X RAY DIFF	2.31	0.27/0.23	C 2 2 21	6.0/689	PHENIX	a=61.14 b=241.44 c=214.83	α=90 β=90 γ=90
5WG5	Transferase	X RAY DIFF	3.10	0.23/0.18	C 2 2 21	6.0/689	PHENIX	a=61.022 b=240.13 c=211.611	α=90 β =90 γ=90
6C2Y	Transferase/ Signalling Protein	X RAY DIFF	2.74	0.29/0.24	C 2 2 21	6.0/689	PHENIX	a=60.55 b=240.45 c=212.76	α=90 β=90 γ=90
6U7C	Transferase/ Signalling Protein	X RAY DIFF	2.44	0.26/0.23	C 2 2 21	6.0/689	PHENIX	a=60.63 b=240.6 c=214.57	α=90 β=90 γ=90
7K7L	Signalling Protein, Transferase/ inhibitor	X-RAY DIFF	2.54	0.24/0.20	C 1 2 1	6.5/640	PHENIX	a=194.39 b=70.76 c=111.23	α=90 β=110.58 γ=90
7K7Z	Signalling Protein, Transferase/ inhibitor	X-RAY DIFF	2.61	0.26/0.20	C 1 2 1	6.5/640	PHENIX	a=194.67 b=70.68 c=111.50	α=90 β=110.46 γ=90

Table 2: *Presence of Unique Conserved Water Molecules in human GRK2 and GRK2 with human $G_\beta G_\gamma$ subunit.*

Human GRK2 (PDB Id. 5UVC)	**Human GRK2 with $hG_\beta G_\gamma$ (PDB Id. 5UKL)**
Unique Water (Water Id)	**Unique Water (Water Id)**
IW1(W702)	IW9(W810)
IW2(W703)	IW10(W814)
IW3(W707)	IW11(W839)
IW4(W709)	IW12(W860)
IW5(W715)	IW13(W866)
IW6(W716)	IW14(W876)
IW7(W734)	IW15(W891)
IW8(W754)	IW16(W928)
	IW17(W931)

Table 3: *Unique conserved water molecules in human GRK2 protein and normalized B-factors with SASA values and H-Bonds of those water molecules.*

Water Id	PDB Id/ Water Id	B-Factor (Å²)	Normalized B-factor	SASA (Å²)		Position of Water	H-Bonds
				SASA Total	SASA Exposed		
IW1	5UVC/W702	25.92	-2.06	107.14	0.00	Buried	4
IW2	5UVC/W703	40.93	-1.16	107.14	0.00	Buried	3
IW3	5UVC/W707	65.62	0.33	107.14	29.79	Semi-Buried	3
IW4	5UVC/W709	51.14	-0.54	107.14	0.00	Buried	1
IW5	5UVC/W715	39.91	-1.22	107.14	30.42	Semi-Buried	6
IW6	5UVC/W716	49.99	-0.61	107.14	43.28	Semi-Buried	3
IW7	5UVC/W734	42.86	-1.04	107.14	0.00	Buried	2
IW8	5UVC/W754	33.50	-1.61	107.14	0.00	Buried	1

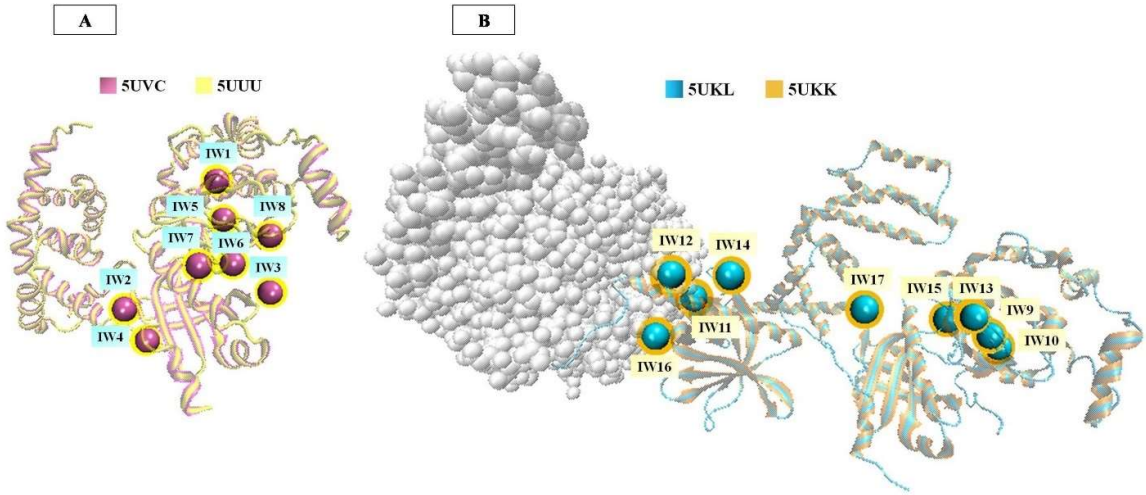

Figure 3: *Superposition X-ray structures reveal the positions of conserved water molecules at the corresponding domain of the hGRK2 protein. (A) Superimposed complexes between PDB Id. 5UVC and 5UUU of category-I water molecules (W1 to W8) and (B) PDB Id. 5UKL and 5UKK of category-II water molecules (W9 to W17).*

Table 4: *Unique conserved water molecules in human GRK2 protein with human $G_\beta G_\gamma$ and normalized B-factors with SASA values and H-Bonds of those water molecules.*

Water Id	PDB Id/ Water Id	B-Factor (Å²)	Normalized B-factor	SASA (Å²)		Position of Water	H-Bonds
				SASA Total	SASA Exposed		
IW9	5UKL/W810	34.06	-1.12	107.14	0.00	Buried	3
IW10	5UKL/W814	33.58	-1.14	107.14	12.00	Buried	3
IW11	5UKL/W839	54.90	-0.27	107.14	0.00	Buried	2
W12	5UKL/W860	33.27	-1.15	107.14	46.71	Semi-Buried	3
W13	5UKL/W866	45.68	-0.65	107.14	9.00	Buried	2
W14	5UKL/W876	39.29	-0.91	107.14	39.85	Semi-Buried	3
W15	5UKL/W891	45.73	-0.64	107.14	46.07	Semi-Buried	3
W16	5UKL/W928	45.68	-0.65	107.14	0.00	Buried	1
W17	5UKL/W931	35.39	-1.06	107.14	57.64	Exposed	3

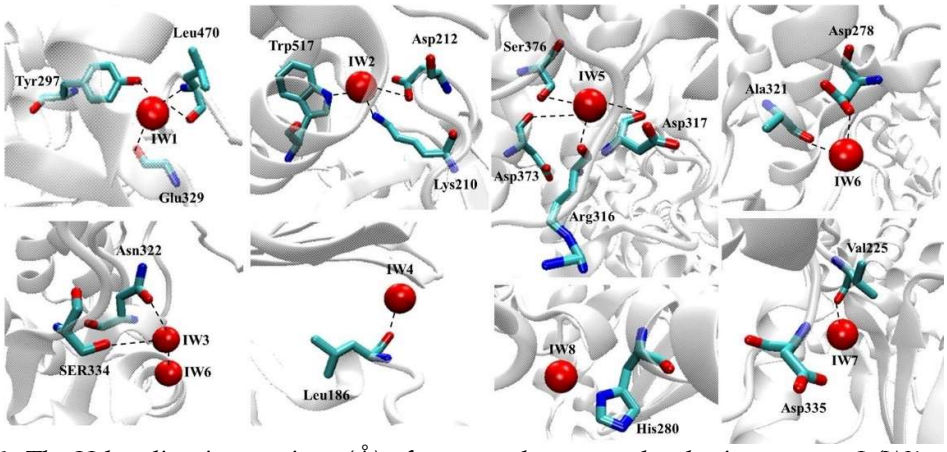

Figure 4: *The H-bonding interactions (Å) of conserved water molecules in category-I (W1 to W8) of crystal structure 5UVC (PDB Id.).*

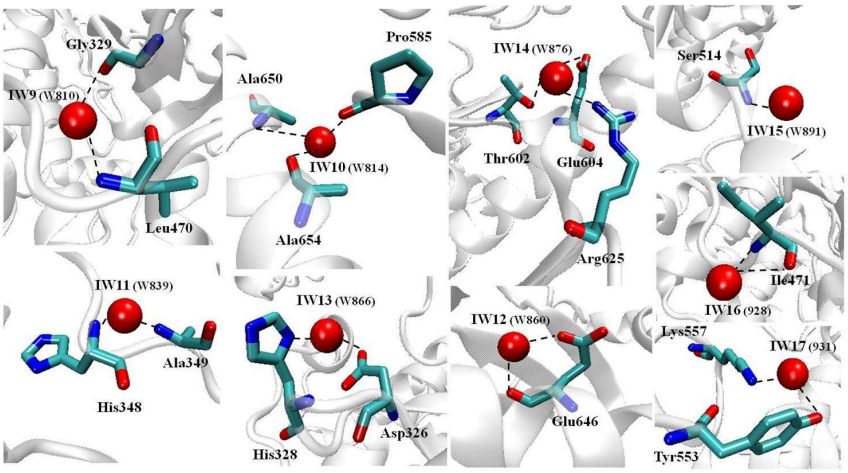

Figure 5: *The H-bonding interactions (Å) of conserved water molecules in category-ii (W9 to W17) of crystal structure 5UKL (PDB Id.).*

The water molecules with a restricted solvent-accessible surface area of less than 20% were considered to be buried water molecules [44] because they are shielded due to other neighboring atoms preventing water from accessing the atom of interest. Therefore, the water molecules IW1, IW2, IW3, IW5, IW6, IW7, IW9, IW10, and IW12 contain SASA values less than 20%, and they are considered stable, invariant, and deeply buried in crystal structures Figure 6 and 7.

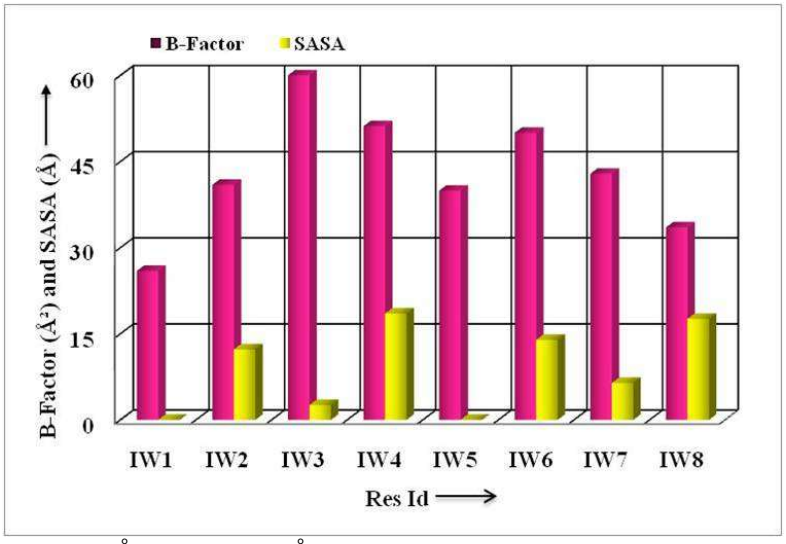

Figure 6: *The B-Factor (Å) and SASA (Å2) value of water molecules (W1 to W8) in human GRK2 without $G_\beta G_\gamma$ subunit.*

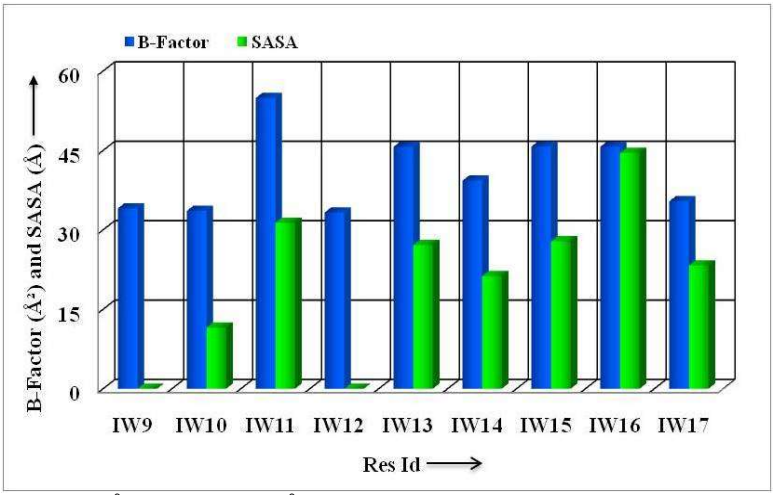

Figure 7: *The B-Factor (Å) and SASA (Å2) value of water molecules of category-II (W9 to W17) in human GRK2 with $G_\beta G_\gamma$ subunit.*

In contrast, the locations of remaining water sites are dynamic and semi or exposed. However, the restricted solvent accessible surface area (SASA) of IW1 and IW10 indicates their structural position in human GRK2 protein is completely buried, whereas IW3 and IW15 are semi-buried. This computational structural data indicates IW1 and IW10 in human GRK2 are tightly bound at their respective hydration sites and may not be displaced during the structural transition. Furthermore, W17 in category II is highly exposed and may easily be displaced. However, the water-mediated slat-bridge interactions are observed in IW2, IW13, and IW14 locations. The water mediated salt bridge interactions are present as Asp212---IW2---Lys210 and Asp326---IW13---His328 in kinase domain and Glu604---IW14---Arg625 in PH domain of GRK2 (Table 5; Figure 8). The IW5 stabilizes four center H-bonds with backbone atoms of the kinase domain in the GRK2 protein. During water dynamics in the presence or absence (only presence of bulk water molecules) of crystal water molecules, we observed **water Id IW1, IW2, IW4, IW5, IW6, IW7, and IW8 of category-I and IW14 and IW16 of category-II** are still available and occupied at the similar position as observed in crystal structures. However, IW9, IW11, and IW13 water sites are found only in water dynamics in the presence of crystal water molecules but unavailable in the presence of bulk water molecules (Table 6 and Figure 9).

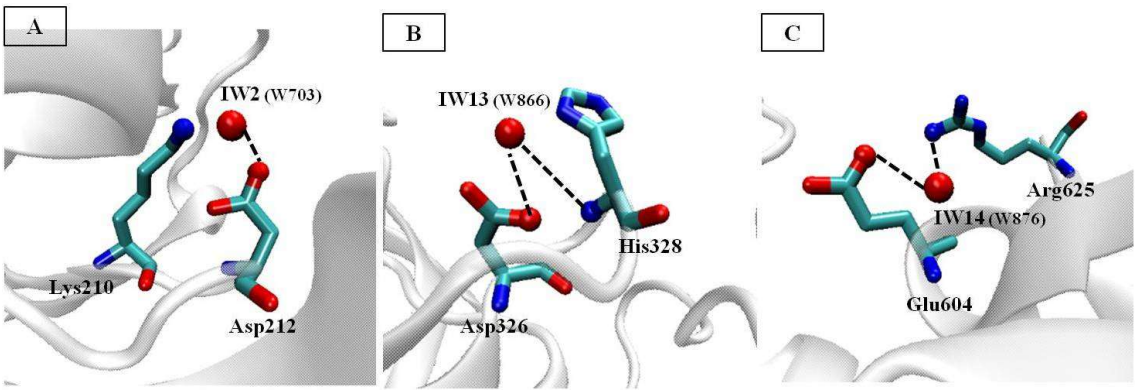

Figure 8: *Conserved water-mediated salt Bridge interactions of IW2, IW13, and IW14. The H-bonding interactions (Å) are (A) Asp212---IW2---Lys210, (B) Asp326---IW13---His328 in kinase domain, and (C) Glu604---IW14---Arg625 in PH domain of hGRK2.*

Table 5: *H-bonding interaction (Å) of water molecules with main chain and side chain of protein residues.*

PDB Id	Number of invariant water molecules		Interaction with main chain atoms	Interaction with side chain atoms	Interaction with water molecules
5UVC	IW1	W702	GLY329 O 2.85 LEU470 O 2.71 LEU470 N 3.32	TYR297 OH 2.63	NA
	IW2	W703	NA	LYZ210 NZ 2.66 ASP212 OD2 2.85 TRP517 NE1 2.77	NA
	IW3	W707	NA NA	ASN322 OD1 3.26 SER334 OG 2.73	W716 3.02 NA
	IW4	W709	LEU186 N 2.75	NA	NA
	IW5	W715	ARG316 O 3.38 ARG316 N 3.40 ASP317 N 3.27	NA ASP373 OD1 2.85 SER376 OG 2.96	NA
	IW6	W716	NA ALA321 O 2.86	ASP278 OD2 3.23	W707 3.02
	IW7	W734	VAL255 O 2.93 ASP335 N 3.38	NA	NA
	IW8	W754	NA	HIS280 ND1 3.23	NA
5UKL	IW9	W810	LEU470 O 2.56 GLY329 O 2.74	 TYR297 OH 2.87	NA
	IW10	W814	PRO585 O 2.76 ALA650 O 2.58 ALA654 N 3.38	NA	NA
	IW11	W839	HIS348 N 2.65 ALA349 N 2.94	NA	NA
	IW12	W860	GLU646 O 2.71	GLU646 OE1 2.85	W100 2.57
	IW13	W866	NA	ASP326 OD1 2.72 HIS328 ND1 2.98	NA
	IW14	W876	NA	THR602 OG1 2.75 GLU604 OE2 2.75 ARG625 NH23.02	NA
	IW15	W891	SER514 N 2.80	NA	W953 3.31 W101 2.73

IW16	W928	NA ILE471 N 2.90	NA	NA
IW17	W931	NA	TYR553 OH 3.13 LYS557 NZ 2.91	W828 3.31
IW19	W816	HIS185 O 3.10 HIS185 N 2.39	NA	W879 3.29
IW20	W840	ASN586 O 2.68 MET603 N 3.07 GLU604 N 3.20	GLU604 CG 3.31	NA
IW21	W849	ASP558 O 2.81	NA	W883 3.17
IW22	W853	MET216 N 2.86	NA	NA
IW23	W861	VAL609 N 3.04 VAL 609 O 3.57	GLU610 OE1 3.27 TYR651 OH 2.98 ARG652 NH2 3.33	NA

Table 6: *The conserved water molecules in crystal and MD simulated structure in human GRK protein (with and without crystal water).*

Water Id	Water Molecules in Crystal Structures	Water Molecules in MD Structures without crystal water molecules	Water Molecules in MD Structures with water molecules
IW1	W702	MD Water	W702
IW2	W703	MD Water	W703/
IW3	W707	Nil	Nil
IW4	W709	MD Water	W709
IW5	W715	MD Water	W715
IW6	W716	MD Water	W716
IW7	W734	MD Water	W734
IW8	W754	MD Water	Nil
IW9	W810	Nil	W810
IW10	W814	Nil	Nil
IW11	W839	Nil	W839
IW12	W860	Nil	Nil
IW13	W866	Nil	W866
IW14	W876	MD Water	W876
IW15	W891	Nil	W891
IW16	W928	MD Water	W928
IW17	W931	Nil	W931

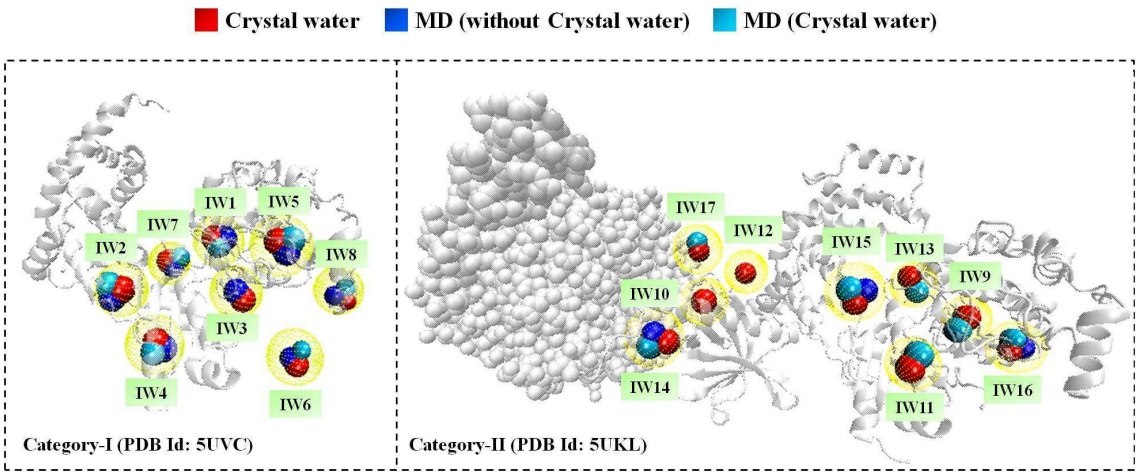

Figure 9: *The superimposed complex structures are crystal and MD conformation (presence and absence of crystal water molecules). The water molecules with red, deep blue, and light blue represents crystal, MD with presence of crystal water, and absence of crystal water molecules respectively.*

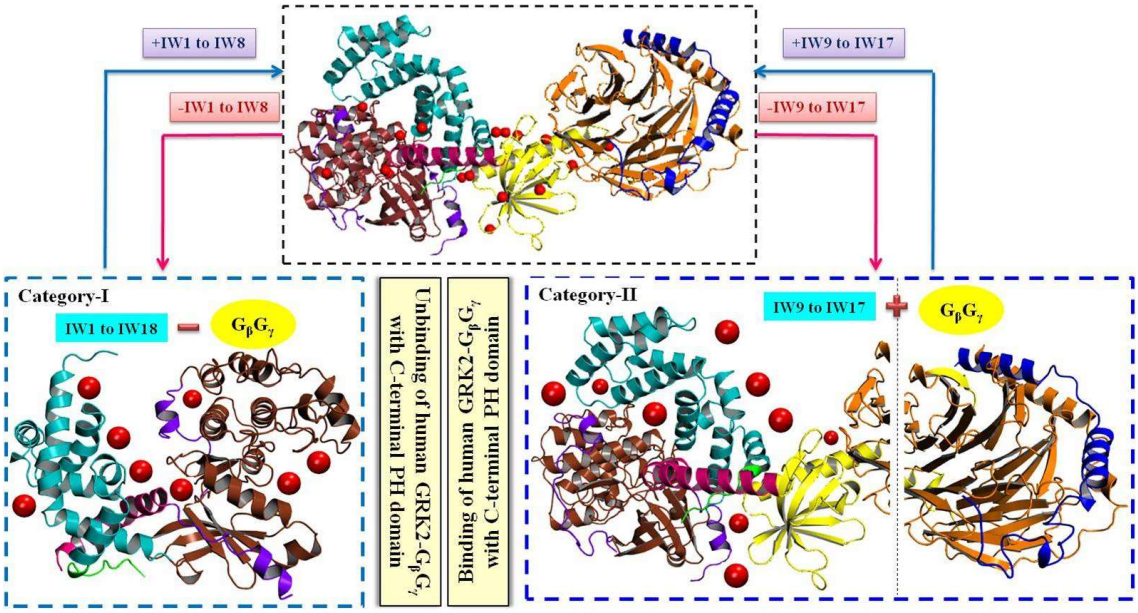

Figure 10: *Conformational transition of human GRK2 from its unbound GβGγ subunit to bound form. The water molecules IW1 to IW8 are departed from the hGRK2 when the $G_\beta G_\gamma$ subunit binds with the C-terminal of the PH domain of GRK2, as well as IW9 to IW17, are entered. The IW9 to IW17 is also leaving when $G_\beta G_\gamma$ free from the PH domain of GRK2.*

4. Conclusion

During the structural transition of human GRK2 from unbound $G_\beta G_\gamma$ to its bound form, IW1 to W17 water molecules play a decisive role in maintaining the structural architecture of human GRK2 protein. The water molecules IW1 to IW8 are departed from the GRK2 kinase domain when the $G_\beta G_\gamma$ subunit binds with the C-terminal of the PH domain of GRK2, as well as IW9 to IW17, are entered. On the contrary, the IW9 to IW17 is also leaving when $G_\beta G_\gamma$ free from the PH domain of GRK2. Analysis of multiple crystal structures reveals the binding and unbinding mechanism of the $G_\beta G_\gamma$ subunit with the C-terminal PH domain of the human

GRK2 protein (Figure 10) may control the opening and closing of these nine hydration sites. Therefore, IW9 to IW17 are the signature hydration sites of the kinase domain that are closely correlated with the $G_{\beta}G_{\gamma}$ subunit. The MD simulation results suggest the non-crystal and crystal water molecules are inaccessible to reaching W3, W10, and W12 water sites because they are deeply buried and shielded by neighboring residues, whereas W9, W11, and W13 are accessible by crystal water in MD simulation but not allow entering non-crystal or MD water molecules. The result of the present study suggests the importance of biochemical information about the association and dissociation mechanism of GRK2 protein with $G_{\beta}G_{\gamma}$ and provides a testable hypothesis for experimental validation.

Acknowledgement

We are very much thankful to the Department of Bioinformatics, Maulana Abul Kalam Azad University of Technology, West Bengal, for providing the computational resources and other infrastructural facilities to conduct the research work.

References

1. Murga C, Arcones AC, Cruces-Sande M, et al. G Protein-coupled receptor kinase 2 (GRK2) as a potential therapeutic target in cardiovascular and metabolic diseases. Front Pharmacol. 2019;10:112.

2. Homan KT, Tesmer JJ. Structural insights into G protein-coupled receptor kinase function. Curr Opin Cell Biol. 2014;27:25-31.

3. Gurevich VV, Gurevich EV. GPCR Signaling Regulation: the role of GRKs and arrestins. Front Pharmacol. 2019;10:125.

4. Ge H, Wang H, Pan B, et al. G protein-coupled receptor (GPCR) reconstitution and labeling for solution nuclear magnetic resonance (NMR) studies of the structural basis of transmembrane signaling. Molecules. 2022;27:2658.

5. Hilger D. The role of structural dynamics in GPCR-mediated signaling. FEBS J. 2021;288:2461-89.

6. Matthees ESF, Haider RS, Hoffmann C, et al. Differential regulation of GPCRs-are GRK expression levels the key? Front Cell Dev Biol. 2021;9:687489.

7. Waldschmidt HV, Homan KT, Cato MC, et al. Structure-based design of highly selective and potent G protein-coupled receptor kinase 2 inhibitors based on paroxetine. J Med Chem. 2017;60:3052-69.

8. Okawa T, Aramaki Y, Yamamoto M, et al. Design, synthesis, and evaluation of the highly selective and potent G-protein-coupled receptor kinase 2 (GRK2) inhibitor for the potential treatment of heart failure. J Med Chem. 2017;60:6942-90.

9. Congreve M, de Graaf C, Swain NA, et al. Impact of GPCR structures on drug discovery. Cell. 2020;181:81-91.

10. Schumacher SM, Gao E, Zhu W, et al. Paroxetine-mediated GRK2 inhibition reverses cardiac dysfunction and remodeling after myocardial infarction. Sci Transl Med. 2015;7:277ra31.

11. Bairagya HR, Tasneem A, Rai GP, et al. Structural and dynamical impact of water molecules at substrate- or product-binding sites in human GMPR enzyme: a study by molecular dynamics simulations. J Phys Chem B. 2021;125:1351-62.

12. Gauto DF, Di Lella S, Guardia CM, et al. Carbohydrate-binding proteins: dissecting ligand structures through solvent environment occupancy. J Phys Chem B. 2009;113:8717-24.

13. Bellissent-Funel MC, Hassanali A, Havenith M, et al. Water determines the structure and dynamics of proteins. Chem Rev. 2016;116:7673-97.

14. Spyrakis F, Ahmed MH, Bayden AS, et al. The roles of water in the protein matrix: a largely untapped resource for drug discovery. J Med Chem. 2017;60:6781-827.

15. Keretsu S, Bhujbal SP, Joo Cho S. Computational study of paroxetine-like inhibitors reveals new molecular insight to inhibit GRK2 with selectivity over ROCK1. Sci Rep. 2019;9:13053.

16. Wu Y, Wang S, Wang H, et al. Selectivity mechanism of GRK2/5 inhibition through in silico investigation. Comput Biol Chem. 2022;101:107786.

17. Rose PW, Prlić A, Altunkaya A, et al. The RCSB protein data bank: integrative view of protein, gene and 3D structural information. Nucleic Acids Res. 2017;45:D271-81.

18. Sumathi K, Ananthalakshmi P, Roshan MN, et al. 3dSS: 3D structural superposition. Nucleic Acids Res. 2006;34:W128-32.

19. Barber RD. Software to visualize proteins and perform structural alignments. Curr Protoc. 2021;1:e292.

20. Chong SH, Ham S. Dynamics of hydration water plays a key role in determining the binding thermodynamics of protein complexes. Sci Rep. 2017;7:8744.

21. Maurer M, Oostenbrink C. Water in protein hydration and ligand recognition. J Mol Recognit. 2019;32:e2810.

22. Banerjee A, Dasgupta S, Mukhopadhyay BP, et al. The putative role of some conserved water molecules in the structure and function of human transthyretin. Acta Crystallogr D Biol Crystallogr. 2015;71:2248-66.

23. Chakrabarti B, Bairagya HR, Mukhopadhyay BP, et al. New biochemical insight of conserved water molecules at catalytic and structural Zn2+ ions in human matrix metalloproteinase-I: a study by MD-simulation. J Mol Model. 2017;23:57.

24. Kanteev M, Goldfeder M, Fishman A. Structure-function correlations in tyrosinases. Protein Sci. 2015;24:1360-9.

25. Carugo O. How large B-factors can be in protein crystal structures. BMC Bioinform. 2018;19:61.

26. Sun Z, Liu Q, Qu G, et al. Utility of B-factors in protein science: interpreting rigidity, flexibility, and internal motion and engineering thermostability. Chem Rev. 2019;119:1626-65.

27. Piskorz TK, De Vries AH, Van Esch JH. How the choice of force-field affects the stability and self-assembly process of supramolecular CTA fibers. J Chem Theory Comput. 2021;18:431-40.

28. Yang J, Anishchenko I, Park H, et al. Improved protein structure prediction using predicted interresidue orientations. Proc Natl Acad Sci USA. 2020;117:1496-503.

29. Al-Baali M, Narushima Y, Yabe H. A family of three-term conjugate gradient methods with sufficient descent property for unconstrained optimization. Comput Optim Appl. 2015;60:89-110.

30. Tripathi A, Mondal R, Lahiri T, et al. TemPred: a novel protein template search engine to improve protein structure prediction. IEEE/ACM Trans Comput Biol Bioinform. 2023;20:2112-21.

31. Laskowski RA, Jabłońska J, Pravda L, et al. PDBsum: structural summaries of PDB entries. Protein Sci. 2018;27:129-34.

32. Lengths M, Angles M. Limitations of structure evaluation tools errat. Quick Guideline Comput Drug Des. 2018;16:75.

33. Aminfar Z, Tohidfar M. In silico analysis of squalene synthase in Fabaceae family using bioinformatics tools. J Genet Eng Biotechnol. 2018;16:739-47.

34. Kosinski J, Cymerman IA, Feder M, et al. A "FRankenstein's monster" approach to comparative modeling: merging the finest fragments of Fold-Recognition models and iterative model refinement aided by 3D structure evaluation. Proteins. 2003;53:369-79.

35. Kumar P, Arya A. Ramachandran Plot: a simplified approach. Pathfind Res Train Found. 2018;1-7.

36. Waterhouse A, Bertoni M, Bienert S, et al. SWISS-MODEL: homology modelling of protein structures and complexes. Nucleic Acids Res. 2018;46:W296-303.

37. Martínez-Rosell G, Giorgino T, De Fabritiis G. PlayMolecule ProteinPrepare: a web application for protein preparation for molecular dynamics simulations. J Chem Inf Model. 2017;57:1511-6.

38. Shukla R, Tripathi T. Molecular dynamics simulation of protein and protein–ligand complexes. In: Singh DB (ed) Computer-Aided Drug Design. Springer, Singapore. 2020.

39. Paquet E, Viktor HL. Molecular dynamics, Monte Carlo simulations, and Langevin dynamics: a computational review. Biomed Res Int. 2015;2015:183918.

40. Kim M, Kim E, Lee S, et al. New method for constant-NTP molecular dynamics. J Phys Chem A. 2019;123:1689-99.

41. Hollingsworth SA, Dror RO. Molecular dynamics simulation for all. Neuron. 2018;99:1129-43.

42. Baltzis AS, Glykos NM. Characterizing a partially ordered miniprotein through folding molecular dynamics simulations: comparison with the experimental data. Protein Sci. 2016;25:587-96.

43. Collier TA, Piggot TJ, Allison JR. Molecular dynamics simulation of proteins. Methods Mol Biol. 2020;2073:311-27.

44. Pradhan MR, Nguyen MN, Kannan S, et al. Characterization of hydration properties in structural ensembles of biomolecules. J Chem Inf Model. 2019;59:3316-29.

Supporting information

Table S1: *The comparative analysis of protonation state, pKa and buried fraction values of ionizable residues in the crystal structure of hGRK-2 in complex with Gβγ and unbound hGRK-2.*

hGRK-2-Gβγ (PDB ID: 5UKL)				hGRK-2 (PDB ID: 5UVC)			
Res. Id	**pKa**	**Protonation**	**Buried**	**Res. Id**	**pKa**	**Protonation**	**Buried**
E639	7.300403	GLP	0.910714	E36	4.625695	GLU	0
E239	6.804964	GLP	1	E48	4.763407	GLU	0
E491	6.047537	GLU	0.085714	E52	4.533301	GLU	0.135714
E300	5.938516	GLU	0.878571	E56	3.745869	GLU	0
E204	5.208301	GLU	0.385714	E77	3.86568	GLU	0
E36	5.055075	GLU	0.475	E78	4.339437	GLU	0
E605	5.051705	GLU	0.646429	E84	4.732052	GLU	0
E653	5.002273	GLU	0.053571	E87	4.862576	GLU	0
E537	4.862337	GLU	0.467857	E88	4.648619	GLU	0
E646	4.855586	GLU	0.496429	E93	3.360905	GLU	0
E426	4.80908	GLU	0.057143	E96	4.564005	GLU	0
E151	4.790188	GLU	0	E107	3.947544	GLU	0
E233	4.777443	GLU	0.114286	E116	4.567371	GLU	0
E515	4.777434	GLU	0.410714	E151	4.605472	GLU	0
E401	4.769433	GLU	0	E152	4.711274	GLU	0
E550	4.724527	GLU	0	E167	4.699161	GLU	0
E167	4.69216	GLU	0	E181	3.855464	GLU	0.771429
E476	4.676057	GLU	0.185714	E204	4.070856	GLU	0.057143
E99	4.660848	GLU	0	E233	4.469683	GLU	0
E107	4.640177	GLU	0	E239	5.333719	GLU	1
E412	4.620888	GLU	0	E291	4.039792	GLU	0.235714
E490	4.620738	GLU	0	E300	5.846997	GLU	0.892857
E130	4.607081	GLU	0	E306	4.411624	GLU	0.510714
E84	4.6068	GLU	0.214286	E327	4.211574	GLU	0.189286
E616	4.606272	GLU	0	E360	3.718391	GLU	0.8
E98	4.580139	GLU	0	E401	4.851031	GLU	0
E48	4.56217	GLU	0.25	E412	4.59832	GLU	0
E52	4.542781	GLU	0.178571	E420	4.456905	GLU	0
E327	4.51421	GLU	0.264286	E426	4.830987	GLU	0.103571
E504	4.495603	GLU	0	E446	3.708623	GLU	0.160714
E56	4.486832	GLU	0	E449	3.006696	GLU	0
E93	4.486228	GLU	0.314286	E504	4.657135	GLU	0
E551	4.452971	GLU	0.535714	E515	4.723847	GLU	0.396429
E87	4.385956	GLU	0.389286	E520	3.679028	GLU	0.857143

E306	4.384544	GLU	0.517857	E523	4.491916	GLU	0.482143
E610	4.333061	GLU	0	E532	4.533289	GLU	0
E78	4.151502	GLU	0.057143				
E96	4.149395	GLU	0				
E420	4.093462	GLU	0				
E152	4.069921	GLU	0.160714				
E595	4.04472	GLU	0				
E446	4.033838	GLU	0.153571				
E181	3.993945	GLU	0.896429				
E604	3.993864	GLU	0.903571				
E532	3.974379	GLU	0				
E100	3.899103	GLU	0				
E291	3.885911	GLU	0.239286				
E88	3.853652	GLU	0.317857				
E593	3.828483	GLU	0.289286				
E360	3.758137	GLU	0.803571				
E116	3.70105	GLU	0				
E589	3.625033	GLU	0.939286				
E520	3.581854	GLU	0.842857				
E611	3.514954	GLU	0.139286				
E77	3.396103	GLU	0				
E523	3.340608	GLU	0.325				
E449	3.276344	GLU	0				
H75	6.088026	HSE	0.085714	H75	6.184551	HSP	0.089286
H122	6.064936	HSE	0.225	H185	6.598754	HSP	0
H131	7.189182	HSP	0	H194	6.023758	HSE	0
H135	6.799664	HSP	0	H262	5.056858	HSD	0.335714
H185	6.728879	HSP	0.396429	H280	5.741843	HSD	0.289286
H194	5.999632	HSD	0	H282	6.211386	HSP	0.335714
H262	4.620911	HSD	0.485714	H286	7.001931	HSP	0.125
H280	5.239597	HSD	0.425	H307	5.013587	HSE	0.614286
H282	5.778426	HSE	0.560714	H309	6.4639	HSP	1
H286	6.920457	HSP	0.139286	H328	6.704682	HSP	0.082143
H307	4.96586	HSE	0.607143	H330	7.641663	HSP	0.460714
H309	6.649808	HSP	1	H348	6.809444	HSP	0
H328	6.743075	HSP	0	H354	6.314492	HSP	0.185714
H330	7.617459	HSP	0.514286	H388	6.169235	HSP	0.303571
H348	6.260421	HSP	0	H394	6.384634	HSP	0
H354	6.765488	HSP	0.228571	H400	6.483648	HSP	0
H388	6.299279	HSP	0.246429				

H394	6.388028	HSP	0				
H400	6.472263	HSP	0				
H549	6.418086	HSP	0.05				
H562	4.718934	HSD	0.764286				
D49	2.213165	ASP	0.092857	D49	3.271351	ASP	0
D70	2.690149	ASP	0.475	D70	3.724278	ASP	0.653571
D110	3.206282	ASP	0	D110	3.559388	ASP	0.357143
D144	3.772468	ASP	0.032143	D144	3.348832	ASP	0
D160	3.546368	ASP	0	D160	3.86457	ASP	0
D169	3.873562	ASP	0.321429	D169	3.583278	ASP	0.035714
D190	2.590545	ASP	0.292857	D190	3.346927	ASP	0.235714
D212	4.279241	ASP	0.667857	D212	4.848957	ASP	0.667857
D223	3.345814	ASP	0.482143	D223	3.845503	ASP	0.096429
D250	4.118131	ASP	0.496429	D250	4.240999	ASP	0.503571
D265	3.806342	ASP	0.146429	D265	3.561632	ASP	0
D272	3.675868	ASP	1	D272	1.771486	ASP	1
D278	6.735358	ASH	0.767857	D278	4.142177	ASP	0.453571
D293	4.372214	ASP	0.178571	D293	4.111453	ASP	0.171429
D317	4.916528	ASP	0.807143	D317	4.760298	ASP	0.7
D326	4.115321	ASP	0.617857	D326	3.781797	ASP	0.546429
D335	3.337685	ASP	1	D335	2.617252	ASP	0.867857
D341	2.937266	ASP	0.117857	D341	3.104501	ASP	0.135714
D369	3.607975	ASP	0.55	D369	3.348176	ASP	0.575
D373	3.174512	ASP	1	D373	3.582977	ASP	1
D398	3.833183	ASP	0	D398	3.427823	ASP	0
D403	4.204042	ASP	0.307143	D403	4.402664	ASP	0.314286
D415	3.720262	ASP	0	D415	3.765158	ASP	0
D432	3.3813	ASP	0	D432	3.756379	ASP	0
D457	3.425233	ASP	0.096429	D457	3.556664	ASP	0
D481	4.343626	ASP	0.203571	D500	3.921401	ASP	0
D484	3.922228	ASP	0	D502	2.947709	ASP	0
D489	4.013233	ASP	0	D527	4.158063	ASP	0.307143
D492	3.57706	ASP	0	D534	3.63502	ASP	0.25
D500	3.953134	ASP	0				
D502	2.814715	ASP	0.05				
D527	4.100606	ASP	0.125				
D534	3.706954	ASP	0.367857				
D552	3.829805	ASP	0.082143				
D558	4.424013	ASP	0.714286				
D635	3.962721	ASP	0.657143				

D637	3.335696	ASP	0.396429				
D49	4.162825	ASP	0.185714				
D70	2.213165	ASP	0.092857				
D110	2.690149	ASP	0.475				
D144	3.206282	ASP	0				
D160	3.772468	ASP	0.032143				
D169	3.546368	ASP	0				
D190	3.873562	ASP	0.321429				
D212	2.590545	ASP	0.292857				
D223	4.279241	ASP	0.667857				
D250	3.345814	ASP	0.482143				
D265	4.118131	ASP	0.496429				
D272	3.806342	ASP	0.146429				
D278	3.675868	ASP	1				
D293	6.735358	ASH	0.767857				
D317	4.372214	ASP	0.178571				
D326	4.916528	ASP	0.807143				
D335	4.115321	ASP	0.617857				
D341	3.337685	ASP	1				
D369	2.937266	ASP	0.117857				
D373	3.607975	ASP	0.55				
D398	3.174512	ASP	1				
D403	3.833183	ASP	0				
D415	4.204042	ASP	0.307143				
D432	3.720262	ASP	0				
D457	3.3813	ASP	0				
D481	3.425233	ASP	0.096429				
D484	4.343626	ASP	0.203571				
D489	3.922228	ASP	0				
D492	4.013233	ASP	0				
D500	3.57706	ASP	0				
D502	3.953134	ASP	0				
D527	2.814715	ASP	0.05				
D534	4.100606	ASP	0.125				
D552	3.706954	ASP	0.367857				
D558	3.829805	ASP	0.082143				
D635	4.424013	ASP	0.714286				
D637	3.962721	ASP	0.657143				
C72	12.36399	CYS	0.807143	C72	12.4409	CYS	0.942857
C120	9.48098	CYS	0.157143	C154	9.968493	CYS	0.339286

C154	10.7284	CYS	0.575	C175	11.51025	CYS	0.689286
C175	12.38782	CYS	0.996429	C208	11.4017	CYS	0.610714
C208	11.53793	CYS	0.65	C221	10.78366	CYS	0.567857
C221	11.12086	CYS	0.728571	C251	10.97368	CYS	0.803571
C251	11.18038	CYS	0.832143	C256	12.04597	CYS	1
C256	12.49425	CYS	1	C340	10.08065	CYS	0.425
C340	10.08413	CYS	0.457143	C379	12.55548	CYS	1
C379	12.8026	CYS	1	C439	11.78971	CYS	0.735714
C439	11.71257	CYS	0.710714				
C559	11.60466	CYS	0.792857				
C619	10.43157	CYS	0.360714				
C634	13.43931	CYS	1				
Y46	10.53935	TYR	0.364286	Y46	10.04874	TYR	0
Y65	14.56266	TYR	0.7	Y65	13.82806	TYR	0.567857
Y86	12.41614	TYR	0.628571	Y86	12.62608	TYR	0.532143
Y92	12.1182	TYR	0.425	Y92	10.12055	TYR	0
Y112	10.50069	TYR	0	Y112	10.47356	TYR	0.060714
Y149	11.67265	TYR	0.614286	Y149	10.57247	TYR	0
Y206	11.62314	TYR	0.385714	Y206	11.75277	TYR	0.053571
Y217	14.85846	TYR	0.857143	Y217	14.80914	TYR	0.882143
Y259	18.52322	TYR	0.985714	Y259	18.12669	TYR	0.975
Y281	11.61146	TYR	0.042857	Y281	10.25481	TYR	0
Y297	13.17111	TYR	0.796429	Y297	12.92035	TYR	0.717857
Y315	16.19227	TYR	1	Y315	15.60262	TYR	1
Y356	12.58847	TYR	0.917857	Y356	13.30642	TYR	0.921429
Y368	11.21678	TYR	0.535714	Y368	11.03344	TYR	0.507143
Y466	10.24482	TYR	0.117857	Y466	9.955212	TYR	0.021429
Y506	12.36617	TYR	0.528571	Y506	11.87558	TYR	0.382143
Y553	14.56431	TYR	0.778571				
Y564	11.92985	TYR	0.492857				
Y580	12.99558	TYR	0.864286				
Y582	13.56498	TYR	0.617857				
Y651	9.89025	TYR	0.189286				
K30	11.28395	LYS	0.203571	K30	10.58576	LYS	0
K31	10.94924	LYS	0	K31	10.60452	LYS	0
K45	10.35842	LYS	0.45	K45	11.21506	LYS	0
K57	10.79897	LYS	0	K57	10.57563	LYS	0
K62	9.637523	LYS	0.360714	K62	10.01546	LYS	0.432143
K90	10.89633	LYS	0.414286	K90	10.43698	LYS	0
K91	11.43258	LYS	0.092857	K91	10.31068	LYS	0

K94	10.24413	LYS	0.135714	K94	10.46995	LYS	0
K115	10.23767	LYS	0	K115	10.67396	LYS	0
K126	10.45422	LYS	0	K164	10.88067	LYS	0
K138	10.45443	LYS	0	K170	9.880181	LYS	0.517857
K139	10.05046	LYS	0	K178	10.35695	LYS	0.771429
K164	11.71055	LYS	0	K210	11.05948	LYS	0.839286
K170	11.10157	LYS	0.435714	K215	10.74871	LYS	0.585714
K178	10.17654	LYS	0.885714	K220	13.37241	LYS	1
K210	11.43351	LYS	0.817857	K224	8.844621	LYS	0.325
K215	11.0783	LYS	0.535714	K225	10.6557	LYS	0
K220	12.49529	LYS	1	K228	11.48313	LYS	0
K224	8.544802	LYS	0.482143	K230	10.07464	LYS	0
K225	10.80653	LYS	0	K266	11.35039	LYS	0.167857
K228	11.1078	LYS	0	K319	10.25526	LYS	0.489286
K230	10.06491	LYS	0.078571	K344	10.4704	LYS	0
K266	11.1826	LYS	0.496429	K345	10.4459	LYS	0
K319	10.40726	LYS	0.657143	K346	10.61235	LYS	0
K344	10.50032	LYS	0	K364	10.44899	LYS	0
K345	10.45274	LYS	0	K383	9.008879	LYS	0.557143
K346	10.61318	LYS	0	K395	10.34	LYS	0
K364	10.41407	LYS	0	K397	9.996412	LYS	0
K383	8.20013	LYS	0.796429	K399	10.3134	LYS	0
K395	9.973457	LYS	0	K448	10.6178	LYS	0.414286
K397	10.24947	LYS	0	K465	10.3279	LYS	0
K399	10.34444	LYS	0				
K448	10.48474	LYS	0.460714				
K465	11.08965	LYS	0				
K494	10.2135	LYS	0				
K497	10.34712	LYS	0				
K540	10.45937	LYS	0.014286				
K541	10.55277	LYS	0				
K543	10.39237	LYS	0				
K545	10.40426	LYS	0				
K557	8.083279	LYS	0.635714				
K567	9.343015	LYS	0.357143				
K615	10.38137	LYS	0				
K618	10.6779	LYS	0.160714				
K623	10.38183	LYS	0				
K628	10.52671	LYS	0.003571				
K644	10.93723	LYS	0.135714				

K645	11.86429	LYS	0.082143				
K663	9.097054	LYS	1				
K665	10.46763	LYS	0.092857				
K667	10.22993	LYS	0.75				
R40	11.65116	ARG	0.5	R40	12.03886	ARG	0.217857
R50	12.49977	ARG	0.139286	R50	12.87329	ARG	0
R69	12.7322	ARG	0.407143	R69	13.50066	ARG	0.517857
R80	16.13839	ARG	0.032143	R80	12.5265	ARG	0
R101	12.29277	ARG	0.153571	R104	13.90707	ARG	0
R104	12.53998	ARG	0.060714	R106	12.77815	ARG	0.353571
R106	13.01832	ARG	0	R158	12.48714	ARG	0.035714
R158	12.34765	ARG	0	R173	12.06886	ARG	0.475
R173	12.6514	ARG	0.628571	R195	12.41599	ARG	0
R195	11.98572	ARG	0.146429	R199	12.47326	ARG	0
R199	12.55548	ARG	0.046429	R209	12.25493	ARG	0
R209	12.30672	ARG	0	R226	12.45199	ARG	0
R226	12.27755	ARG	0.342857	R240	11.21988	ARG	0.478571
R240	11.16567	ARG	0.453571	R295	11.7269	ARG	0.353571
R295	11.7538	ARG	0.364286	R311	11.97206	ARG	0.235714
R311	11.89853	ARG	0.271429	R316	12.76138	ARG	0.639286
R316	12.59365	ARG	0.675	R332	13.19519	ARG	0.907143
R332	13.06105	ARG	0.917857	R386	12.06369	ARG	0.089286
R386	12.16168	ARG	0.046429	R392	12.1494	ARG	0.075
R392	12.1133	ARG	0.214286	R404	12.57743	ARG	0
R404	12.54351	ARG	0	R422	12.39488	ARG	0
R422	12.42108	ARG	0	R431	11.00761	ARG	0.532143
R431	12.32492	ARG	0	R435	12.57703	ARG	0
R435	12.53706	ARG	0	R436	13.09028	ARG	0.875
R436	13.12157	ARG	0.878571	R442	13.48623	ARG	0
R442	13.20546	ARG	0	R454	12.49683	ARG	0
R454	12.46029	ARG	0	R474	12.44994	ARG	0
R474	12.44541	ARG	0	R507	12.3665	ARG	0
R507	12.66368	ARG	0	R516	15.51916	ARG	0.932143
R516	14.13509	ARG	0.760714	R535	12.45042	ARG	0
R535	12.41634	ARG	0				
R539	12.19663	ARG	0				
R578	13.53068	ARG	0.385714				
R579	12.161	ARG	0.089286				
R587	13.47221	ARG	1				
R591	14.76705	ARG	0.496429				

R617	12.37732	ARG	0.225
R625	12.16663	ARG	0.45
R648	12.32008	ARG	0.039286
R652	13.20406	ARG	0
R660	12.22919	ARG	0
R669	13.26389	ARG	0.35